TECHNICAL PAPER

CrossMark

Liquefaction potential assessment of Guwahati city using first-order second-moment method

Longbir Singnar[1] · Arjun Sil[1]

Abstract

Soil liquefaction is the failure of the soil due to the sudden increase in a pore water pressure causing the effective stress to reduce significantly thus losing shear strength, with the resulting effect causing the fluid type behavior of the soil. Guwahati city, the capital of Assam, lies in the northeastern region of India and this whole region is considered seismically very active (seismically sixth position globally). The whole region is categorized in Zone-V according to the seismic zoning map of India as per IS 1893:2002 (Part 1). This region witnessed/experienced several major and great earthquakes in the past such as 1897 Shillong and 1950 Assam earthquakes. The soil deposits of the city mainly consist of an alluvial type of Holocene age and the presence of shallow groundwater table makes it vulnerable to soil liquefaction. In this study, an assessment of soil liquefaction potential of Guwahati city is performed based on the methods proposed by Youd and Idriss (J Geotech Geoenviron Eng 127:297, 2001) and Idriss and Boulanger (2010; CPT- and SPT-based liquefaction triggering procedures, 2014) using standard penetration test data. The evaluation of liquefaction potential is carried out for 82 borehole sites considering the Great 1897 Shillong earthquake of M_w 8.1 with a peak ground acceleration of 0.36 g. In the deterministic approach, the various parameters are involved in the evaluation of liquefaction potential, and the uncertainties of the input parameters as well as model cause the dissimilarity of the result. For instance, the same input parameters for both the models show different factor of safety. Hence, a comprehensive probability approach considering the uncertainty of parameters is essential for the evaluation of liquefaction susceptibility. In this study, reliability analysis for both the models based on first-order second-moment method has been used. The Reliability Index based on input parameters such as cyclic resistance ratio and cyclic stress ratio computed for both the models and subsequent liquefaction probability are established. The result shows the city is in most vulnerable condition even up to 15 m depth considering both the methods proposed by Youd and Idriss (J Geotech Geoenviron Eng 127:297, 2001) and Idriss and Boulanger (2010; CPT- and SPT-based liquefaction triggering procedures, 2014). Therefore, extra measure should be taken while constructing structure in and around the study area.

Keywords Soil liquefaction · SPT · Peak ground acceleration · Reliability Index

Introduction

Soil liquefaction is the sudden loss of shear strength of the saturated granular cohesionless soil during earthquake essentially due to the significant swelling in the pore water pressure under the influence of cyclic loading generated in the presence of incoming stress waves reaching at the site from a seismic source (epicenter) suddenly in the form of seismic loading. However, the sudden increase in pore pressure results in the displacement of soil particles, thus behaving like a fluid. Soil liquefaction is generally observed in case of sandy soil or silty sands; however, the clayey soil may also undergo colossal deformation/spreading. For the initiation or triggering of soil liquefaction, it requires a certain level of lateral force generated by the earthquake with reasonable magnitude size, duration and the peak ground acceleration of the earthquake. Conversely, liquefaction could cause severe damage to the structure due to the loss of shear strength of the soil that eventually leads to the foundation failure of the structure. The failure of the soil may be in the form of settlement of the soil, sand boil, and lateral spreading. Since the devastating effect of soil liquefaction observed in 1964 Niigata earthquake, Japan (M_w 7.5), Alaska earthquake in

✉ Arjun Sil
silarjun@gmail.com

[1] NIT Silchar India, Silchar, Assam, India

1964 (M_w 9.2), Loma Prieta Earthquake, USA, in 1989 (M_w 6.9), Kobe Earthquake, Japan, in 1995 (M_w 6.9), Chi–Chi Earthquake, Taiwan, in 1999 (M_w 7.6) and Bhuj Earthquake, India, in 2001 (M_w 7.7), several researchers attempted to develop a technique to evaluate liquefaction potential. Seed and Idriss [1] developed a procedure known as "Simplified procedure" which has been popularly used around the world. Since then, various methods were proposed [2–5, 6]; however, the approach is based on the quantification of cyclic stress/loading generated during an earthquake. To evaluate the actual stress induced in the soil become complex due to the variability of seismic loading and also the uncertainties in the inherent properties of soil [7]. The availability of field data from earlier liquefied sites such as Niigata earthquake and Alaska earthquake enables the researchers to devise an approach to assess liquefaction potential. In the deterministic approach, cyclic stress ratio (CSR) and cyclic resistance ratio (CRR) of the soil are evaluated based on the various geotechnical data, such as standard penetration test (SPT)-N values, properties of soil, and considering the level/status of groundwater table. However, the liquefiability of soil is usually established by its factor of safety representing the ratio of CRR over CSR. However, due to the inherent uncertainty of the parameters disparity exists for various models despite the same input. The development of a probabilistic approach by several researchers takes into account the model uncertainty and parameter uncertainties. Using various mathematical models, a number of probabilistic methods have been developed. Idriss and Boulager [2, 6] specified an updated procedure for probabilistic approach using cone penetration test (CPT)-based case history data, employing limit state function and likelihood function for determining the liquefaction probability. However, reliability approach assists in the evaluation of liquefaction potential by considering the uncertainties in various parameters and describes the nature of variability of the factors involved [8]. In the deterministic approach, the evaluation of liquefaction in terms of probability/uncertainty could not be calculated, it only distinguishes liquefiable and non-liquefiable based on factor of safety. To account uncertainty, Hwang et al. [9] and Jha and Suzuki [10] described the use of reliability approach in the evaluation of liquefaction potential based on SPT data.

In this study, the evaluation of liquefaction potential is carried out based on the first-order second-moment method (FOSM) for the capital city Guwahati, Assam, India. However, considering the geological and topographical aspects, the city is located on the southern bank of the Brahmaputra River in the Kamrup district of Assam. It is also considered as the gateway to the northeastern part of India. The city serves as a center for trade and commerce, education, industry and also connects the rest of India with the northeastern region. The city (approx) covers an area of 216 km^2 having a population of about 9,35,752 (2011 Census). The city is surrounded by hills and inselbergs, to its west lies with the Nilachal hill on the southern banks of the Brahmaputra, the north consists of Chitrachal hill and to the south lies the Narakasur hill. However, seismically Guwahati city lies in Zone-V as per IS 1893:2002 (Part 1) and is considered to be the most seismically active zone with assigned peak ground acceleration (PGA) of 0.36 g. In the past years, the city experienced some great and major earthquakes (1869 Cachar earthquake M_w 7.6, 1897 Great Shillong earthquake M_w 8.1, 1918 Srimangal earthquake M_w 7.5, and 1950 Great Assam earthquake M_w 8.5) [11]. The soil deposits of Guwahati city are mainly the alluvial type deposited in the low-lying area of the city consisting mainly of pebbles, loose sand, silt and clay which are prone to soil liquefaction. In recent years, there has been a rapid increase in the construction of residential buildings, flyovers, and malls around Guwahati city. It is evident in the near future that the expansion of the city's infrastructure would continue to develop. It is, therefore, highly important for the comprehensive assessment of the sites, ensuring the safety and stability of the structures from its catastrophic failures due to uncertain seismic loading. In this study, a total of 82 SPT borehole data at various locations around the city are considered for the evaluation of soil liquefaction based on semi-empirical correlation and reliability approach. The map showing the locations of the borehole in the city area is given in Fig. 1.

Topography and geology

Guwahati city is situated in the Kamrup district of Assam. The city is to be found on the bank of river Brahmaputra placed in the undulating plain with varying altitudes of 49.5–55.5 m above mean sea level (MSL). The overall topography of the greater Guwahati region consists of several continuous hill tracts whose altitude varies from 200 to 400 m above MSL consisting of an isolated hill or inselberg blocks up to 300 m above MSL. The city is situated on the southern banks of the river Brahmaputra and separated by isolated hillocks such as Nilachal hill located in the west of the southern banks of the Brahmaputra, the Chitrachal hill in the north and Narakasur hill in the south. Apart from the hilly tracts, swamps, marshes and small water bodies such as Deepar beel, Dighali Pukhuri and Silsakoo beel also cover the city. The hills surrounding Guwahati city are mostly composed of porphyritic granites and quartzo-feldspathic gneiss that transversely cut by amphibolite intrusive and quartz veins. Sandy soils formed by the weathering of porphyritic granites are found in many areas of the city. The area consists of two main geological formations: (a) Precambrian granitic rocks forming the hill tracts and isolated hillocks; (b) quaternary alluvium occupying the valleys. Alluvial soil of Holocene age is found in the valleys and low-lying areas
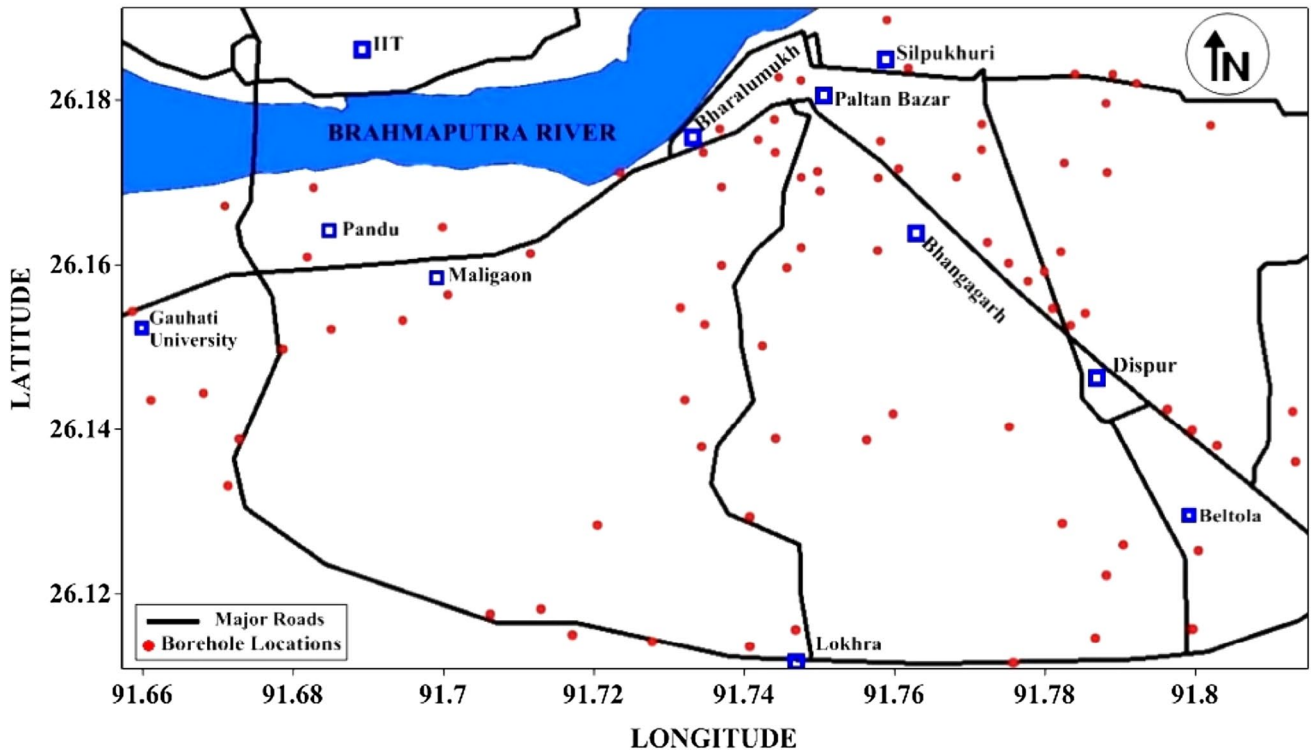
Fig. 1 Map showing borehole locations around Guwahati city

of the city. The newer alluvium deposit could be found up to 20 m depth. They are generally brown- and gray-colored silty clays or clayey silts. At present, most of the prehistoric alluvial soils are overlain by unnaturally transported soil and overburden material brought about by anthropogenic activities. They are visible only in excavations and borings. There is significant variation in the thickness of these layers. The fine-grained fraction mostly comprises soils of classification CL, CI and CH according to the Indian standard soil classification. In a few locations, the inorganic silt having classification ML and CL–ML and non-plastic inorganic silts were also encountered. The coarse-grained fraction generally has classifications such as SP, SW, SC, SM, and SP–SC; however, gravel deposits are also encountered in certain boreholes. However, another important aspect that contributes to liquefaction potential is the geologic age of deposits/sediments. The aging effects of soil initially reported by Youd and Hoose [12] and Youd and Perkins [13] shows that the soil liquefaction resistance of sand increases with the geologic age. They observed that younger soil deposits which are few 100 years become more susceptible to liquefaction than older Holocene sediments (< 10,000 years). The basic mechanism of reduction of liquefaction susceptibility with age reported by Youd and Hoose [12] is the changes of cementing and compaction property of soil through natural process as well as changes in topography, sedimentation process, effect of changes of water table depth, and depth

of burial due to post-depositional geologic process. However, Mitchell [14] and Mitchell and Solymar [15] reported that effect of aging is the result of chemical process such as the formation of silica acid gel on contact particle surfaces through precipitating silica from solution and causing cementing bonds at inter-particle contacts. However, Schmertmann [16] presented that the aging effects are the results of increased in situ effective stresses including grain slippage, dispersive particle movements, increased grain interlocking and internal stress arching. However, considering geologic time, chemical cementation may become more significant. Therefore, it could be concluded that the geologic age contributes in reducing liquefaction susceptibility over a deposit after a long period.

However, in the present study, an attempt has been made to assess probabilistic liquefaction susceptibility considering the available SPT-*N* bore log data (generally represents actual depositional status or stiffness for a long time) based on both the standard methods proposed by Idriss and Boulanger [2, 6] and Youd and Idriss [5] in and around Guwahati city to examine the present status in terms of FOS and Liquefaction Potential Index (LPI) irrespective of geologic aging considering uncertainty. However, based on this study, it has been found that the city becomes highly susceptible in liquefaction even up to 15 m depth and, therefore, the authors believe that geologic age may contribute minimum

effects in this area for improvement of liquefaction resistance of soil.

Seismicity and seismotectonics

The entire northeastern region of India is considered to be the most seismically active zones in the world. Guwahati city is in the lap of the northeast region of India, surrounded by the Himalayan mountain belt in the north, Mishmi hills in the west, the Naga Patkoi mountain range in the south and the Assam valley in the middle, along with the Shillong plateau, the Burmese arc, the Tripura folded belt, and the Bengal Basin and has a very complex tectonic setting. A seismicity map of Northeast India is shown in Fig. 2. However, in past years, the city experienced two great and several major earthquakes. The Great Shillong earthquake (M_w 8.1) which occurred on 12th June 1897 produced by the south dipping hidden fault at the northern boundary of the Shillong plateau known as 'Oldham fault' caused significant damaged in Shillong [11]. Due to the close proximity of Guwahati city to the epicenter (approx. 50 km), significant damage was observed around Guwahati city. After a gap period of about 50 years, on 15th August 1950, the great
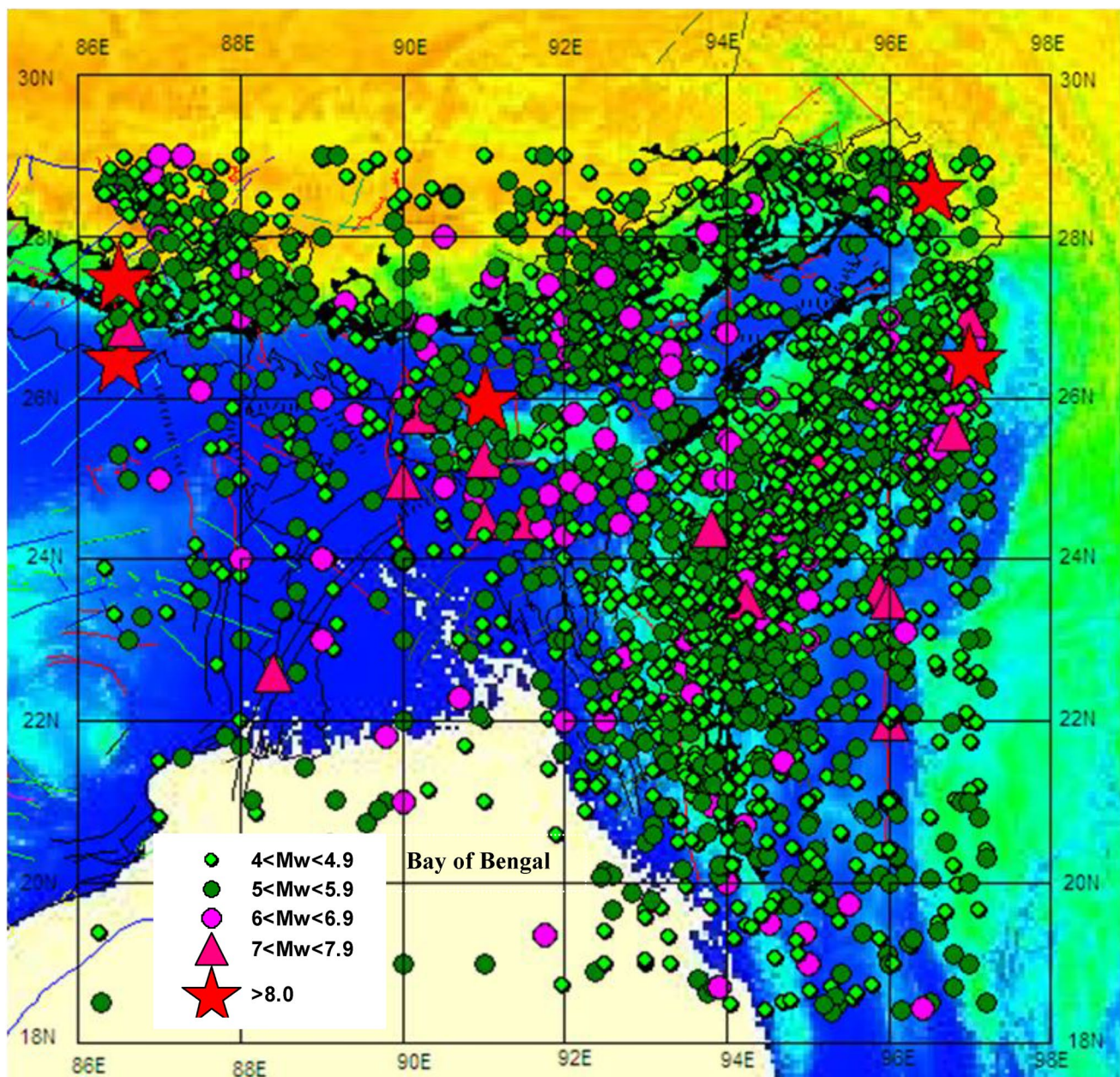

Fig. 2 Seismicity map of Northeast India [17]

Assam earthquake struck the region with M_w 8.5 that caused severe damage, especially in upper Assam but due to a larger epicentral distance of about 600 km, no significant damage was found in Guwahati city. Most of the events falling in the tectonic domains of the eastern Himalaya, Mishmi block, Assam shelf, Meghalaya Plateau and Mikir Hills, Surma and Bengal basins mostly have shallow focal depth, i.e., < 70 km. Indeed, a shallow depth earthquake is severe in nature as the intensity of surface shaking increases with decreases in the depth of focus of an earthquake. Since the last 1897 Great Shillong earthquake, there has been no significant seismic activity in the Shillong plateau. It is expected that in the near future there is a possibility of occurrence of earthquake ($M > 8$) [18, 19]. Gupta and Singh [20] on the basis of P-wave travel-time residuals described that the Shillong plateau experiencing dilatancy stage, a preliminary indication of the possible large earthquake. Guha and Bhattacharya [21], Bilham and England [22] have reported the likelihood of occurrence of a major earthquake ($M > 8$) in the Northeast part of India in near future.

Methodology

The assessment of liquefaction potential for Guwahati city carried out based on the deterministic approach considering both Idriss and Boulanger [2, 6] and Youd and Idriss [5] models and subsequently reliability analysis were performed. In this study, the sites with clay or plastic silt deposition have been avoided for liquefaction evaluation. In this study, a total of 82 borehole SPT data have been assessed. It is normally observed that a soil possessing plasticity is resistant to liquefaction although a large straining of the soil may occur in an event of an earthquake. However, both the methods are described as follows.

Youd and Idriss [5]

The method is based on the recommendation and augmentation of various updates on the previous simplified procedure (Seed'85) for the evaluation of liquefaction potential of the soil. In 1996 and 1998 National Center for Earthquake Engineering Research workshops, several noted researchers and engineers agreed on the update of various parameters and incorporated in the model for the use in routine practice. However, liquefaction is evaluated based on comparing the cyclic stress induced in the soil due an earthquake and the cyclic resistance of the soil. The method is based on Seed'85 procedure in which various parameters were updated. However, magnitude scaling factor, overburden correction factors were reviewed and the evaluation of liquefaction potential using CPT as well as Becker penetration test has been reviewed.
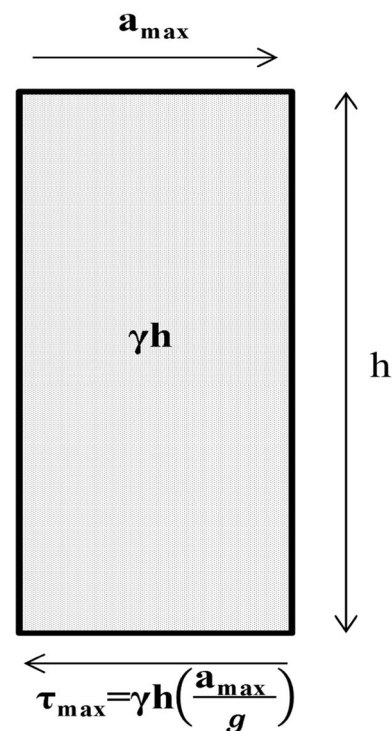
Fig. 3 Typical schematic for determining the maximum stress

In liquefaction assessment, the CSR which represents the stress demand in the soil for the initiation of liquefaction could be expressed as the ratio of maximum stress, τ_{max}, (Fig. 3) over effective overburden pressure σ_v'. The cyclic stress induced in the soil is mostly influenced by the shaking due to an earthquake [23]. In the present study, PGA of 0.36 g is being considered for the assessment.

The CSR is computed using the following equation by Seed and Idriss [1]:

$$(CSR)_{M=7.5, \sigma=1} = 0.65 \left(\frac{\sigma_{vo} a_{max}}{\sigma_{vo}' g} \right) \frac{r_d}{\text{magnitude scaling factor (MSF)}}, \tag{1}$$

CSR is computed corresponding to the effective stress of 1 atm, σ_{vo} is the total overburden pressure, σ_{vo}' is the effective overburden pressure, r_d is the stress reduction factor, a_{max} peak horizontal acceleration at the ground surface and g acceleration due to gravity.

Considering for the flexibility of soil column, the stress reduction factor (r_d) is employed for stress reduction. The reduction factor, r_d, varies with depth and it equals to one at the ground surface. The following equations are recommended to estimate the average values of r_d [24]:

$$r_d = 1.0 - 0.00765Z \quad \text{for } (Z \le 9.15), \tag{2a}$$

$$r_d = 1.174 - 0.0267Z \quad \text{for } (9.15 \le Z \le 23), \tag{2b}$$

where Z is the depth in meters.

The CRR was based on the empirical relation for earthquake magnitude $M_w = 7.5$. For magnitude other than 7.5, a MSF is used which represents the number of equivalent cyclic stress required to cause liquefaction. As per Youd and Idriss [5], the following MSF is recommended:

$$\text{MSF} = \frac{10^{2.24}}{M_w^{2.56}}. \tag{3}$$

The CRR is defined as the resistance of the soil to resist liquefaction. For the computation of CRR, parameters such as relative density, D_r, and in situ stress are required which cannot be retrieved with the typical drilling and sampling techniques. It involves the application of sophisticated sampling procedure such as ground freezing, which could extract the undistorbed sample required for laboratory testing. The cost of employing such technique is highly uneconomical.

Indeed, for several years, the field tests have been used to establish the relationship with the CRR. The SPT is commonly used for determining the resistance of the soil characterized by the N values obtained. The N values observed are corrected for overburden pressure of approximately 100 kPa and other correction factors are applied using the following equation:

$$(N_1)_{60} = N C_N C_E C_B C_R C_S, \tag{4}$$

where N is the no. of blows observed, C_E hammer efficiency, C_B correction for borehole diameter, C_R correction for rod length, C_S correction for sampler with or without liner and C_N is the overburden stress correction factor computed using the given relation [25]:

$$C_N = \sqrt{\frac{P_a}{a'_{vo}}} \le 1.7, \tag{5}$$

where P_a is equal to approximately 100 kPa.

The corrected N values, i.e., $(N_1)_{60}$ are further corrected for fine content, as cohesionless soil containing higher fine content, FC, results in increases of penetration resistance.

The following relation is used for fine content for correction $(N_1)_{60}$ to an equivalent clean sand value $(N_1)_{60cs}$:

$$(N_1)_{60cs} = \alpha + \beta (N_1)_{60}, \tag{6}$$

where α and β are coefficients determined from the following relationships:

$$\alpha = 0, \ \beta = 1 \quad \text{for (FC} \le 5\%), \tag{6a}$$

$$\alpha = \exp\left[1.76 - \left(\frac{190}{\text{FC}^2}\right)\right],$$

$$\beta = \exp\left[0.99 + \left(\frac{\text{FC}^{1.5}}{1000}\right)\right] \quad \text{for (5\% } \le \text{FC} \le 35), \tag{6b}$$

$$\alpha = 5, \ \beta = 1.2 \quad \text{for (FC} > 35\%). \tag{6c}$$

The computation for CRR of cohesion less soil containing any fine content is given by the following expression:

$$\text{CRR}_{M=7.5} = \frac{1}{34 - (N_1)_{60cs}} + \frac{(N_1)_{60cs}}{135} + \frac{50}{[10(N_1)_{60cs} + 45]} - \frac{1}{200}. \tag{7}$$

This equation is valid for $(N_1)_{60cs} < 30$. For $(N_1)_{60cs} \ge 30$, clean granular soils are too dense to liquefy and are classified as non-liquefiable. The evaluation of liquefaction is based on the factor of safety, which is the ratio of CRR upon the CSR, factor of safety (FS) $= \left(\frac{\text{CRR}_{M=7.5}}{\text{CSR}}\right) K_\sigma K_\alpha$,

where K_σ is the overburden correction factor for CRR and K_α is the correction for sloping ground.

The application using K_σ and K_α is beyond routine practice and requires special expertise. However, it could be used in the hazard analysis of embankment dams or other large structures.

Idriss and Boulanger [2, 6]

Idriss and Boulanger [6] describe about the correlation of liquefaction with standard penetration N values. In this method, new case history was updated providing detailed illustration of liquefaction triggering correlation. Several parameters were improved such as stress reduction coefficient r_d, MSF, overburden correction factor K_σ for CSR, and overburden correction factor C_N for penetration resistances based on new case history. However, due to the availability of new data and cases, the method has undergone several changes.

However, according to Idriss and Boulanger [2], the report mostly contains revised liquefaction triggering procedure for the CPT-based method. However, significant case history data were added to the SPT-based method also. The important features of the newly revised report include the relationship of MSF with liquefaction for SPT- and CPT-based procedures. The recently developed MSF has included the soil types in its applications to the evaluation of the CSR. In the earlier methods, the uses of MSF are limited to only clean sands, but the newly formulated MSF could be applied to the various soil types. For sand, clay and plastic silt, different MSF has been established.

The CSR is given as [1]:

$$(\text{CSR})_{M=7.5, \, \sigma=1 \, \text{atm}} = 0.65 \cdot \left(\frac{\sigma_{vo}}{\sigma'_{vo}} \cdot \frac{a_{max}}{g}\right) \frac{r_d}{\text{MSF}}, \tag{8}$$

σ_{vo} is the total overburden pressure, σ'_{vo} is the effective overburden pressure, a_{max} is the maximum horizontal

acceleration at the ground surface, MSF is the magnitude scaling factor and r_d is the stress reduction factor.

The MSF is included to account for duration effects (i.e., number of loading cycles) and magnitude on the triggering of liquefaction. Earlier, the MSF developed by various researchers proposed the same MSF for all types of soil. The MSF expression as per Idriss and Boulanger [6] was dependent on magnitude of earthquake only, which is same as their predecessor (Eq. 9a). However, Idriss and Boulanger [2] developed a new MSF (Eq. 9b), the new MSF was developed for sandy, clay and plastic silt types of soil. The MSF was used to account for duration effects (i.e., number of loading cycles) on the triggering of liquefaction. It could be computed using the following equation:

$$MSF = 6.9 \exp\left(\frac{-M}{4}\right) - 0.058 \le 1.8, \tag{9a}$$

$$MSF = 1 + (MSF_{max} - 1)\left\{8.64 \exp\left(\frac{-M}{4}\right) - 1.325\right\}, \tag{9b}$$

where $MSF_{max} = 1.8$ for sand and $MSF_{max} = 1.09$ for clay and plastic silt. Also the MSF_{max} relationship with $(N_1)_{60cs}$ can be established as:

$$MSF_{max} = 1.09 + \left(\frac{(N_1)_{60cs}}{31.5}\right)^2 \le 2.2. \tag{9c}$$

Response reduction factor, r_d, which accounts for the dynamic response of the soil profile as per Idriss and Boulanger [2] is given as:

$$\ln(r_d) = \alpha(Z) + \beta(Z)M, \tag{10a}$$

$$\alpha(Z) = -1.012 - 1.126 \sin\left(\frac{Z}{11.73} + 5.133\right), \tag{10b}$$

$$\beta(Z) = 0.106 + 0.118 \sin\left(\frac{Z}{11.28} + 5.142\right), \tag{10c}$$

where Z is depth in meters and M is moment magnitude. These equations are applicable to a depth $Z \le 34$ m, whereas the following expression is applicable for $Z > 34$:

$$r_d = 0.12 \exp(0.22M). \tag{11}$$

The soil CRR is usually correlated to an in situ parameter such as SPT blow count. The SPT blow counts are affected by a number of procedural details (rod lengths, hammer energy, sampler details, and borehole size) along with effective overburden stress. Thus, the correlation to CRR is based on corrected penetration resistance:

$$(N_1)_{60} = C_N C_E C_B C_R C_S N_m, \tag{12}$$

where C_N is an overburden correction factor, C_E is hammer efficiency, C_R is a rod correction factor to account for

energy ratios being smaller with shorter rod lengths, C_B is a correction factor for borehole diameters, C_S is a correction for sampler, and N_m is the measured SPT blow count. The CRR is also affected by the duration of shaking (which is correlated to the earthquake MSF and effective overburden stress expressed through a K_σ factor). The correlation for CRR is, therefore, developed for a reference $M_w = 7.5$ and $\sigma'_v = 1$ atm, and then adjusted to other values of M and σ'_v using the following expression:

$$CRR_{M,\sigma} = CRR_{M=7.5, \sigma=1\,atm} \cdot MSF \cdot K_\sigma. \tag{13}$$

C_N is an overburden correction factor is given as:

$$C_N = \left(\frac{P_a}{a'v_0}\right)^\alpha \le 1.7, \tag{14a}$$

$$\alpha = 0.784 - 0.0768\sqrt{(N_1)_{60}}, \tag{14b}$$

K_σ overburden correction factor for CRR, which is expressed as:

$$K_\sigma = 1 - C_\sigma \ln\left(\frac{\sigma'v_0}{P_a}\right) \le 1.1, \tag{15a}$$

$$C_\sigma = \frac{1}{18.9 - 2.25\sqrt{(N_1)_{60}}}. \tag{15b}$$

The correlation between the CRR adjusted to $M = 7.5$ and $\sigma'_v = 1$ atm and the equivalent clean sand $(N_1)_{60cs}$ value for cohesionless soils is given by the following expression:

$$CRR = \exp\left\{\frac{(N_1)_{60cs}}{14.1} + \left(\frac{(N_1)_{60cs}}{126}\right)^2 - \left(\frac{(N_1)_{60cs}}{23.6}\right)^3 + \left(\frac{(N_1)_{60cs}}{25.4}\right)^4 - 2.8\right\}. \tag{16}$$

The equivalent clean sand adjustment developed by Idriss and Boulanger [6] is expressed as:

$$(N_1)_{60cs} = (N_1)_{60} + \Delta(N_1)_{60}, \tag{17}$$

$$\Delta(N_1)_{60} = \exp\left(1.63 + \frac{9.7}{FC + 0.01} - \left(\frac{15.7}{FC + 0.01}\right)^2\right). \tag{17a}$$

The factor of safety against soil liquefaction is given by $FS = \frac{CRR_{M=7.5}}{CSR}$.

The computation of FS based on the method by Idriss and Boulanger [2, 6] and Youd and Idriss [5] is shown in Tables 1 and 2, respectively. A comparison of a FS between the two methods is shown in Fig. 4.

Table 1 Typical computation of FS for PGA = 0.36 g corresponding to M_w = 8.1 based on (a) Idriss and Boulanger [6], (b) Idriss and Boulanger [2]

Location :   Rehabari. GWT:1.3m
Bore Hole_ID:K14.1 Lat- 26.17 °   Long-91.75 °   **(a)**

Depth (m)	Soil Description	Lithology	N_{obs}	Fines Content %	$?_v$ (kN/m^2)	$?_v'$ (kN/m2)	N_{cr}	R_d	CSR	CRR	FS
1.5			8	-	26.16	24.20	12				
3	Clay upto	■	19	-	70.27	53.59	19				
4.5	8m		19	-	114.38	82.99	18				
6			15	-	158.49	112.38	12				
7.5			11	-	202.60	141.78	10				
9			13	-	247.13	171.59	10	0.931	0.390	0.125	0.321
10.5	Silt and Fin		25	4.8	291.85	201.60	18	0.894	0.403	0.192	0.476
12	Sand from		28	4.7	336.56	231.59	19	0.854	0.409	0.207	0.506
13.5	8m to 9m		29	3.6	381.28	261.60	19	0.814	0.410	0.202	0.493
15			26	3.8	425.99	291.59	16	0.774	0.403	0.168	0.417

Location :   Rehabari. GWT:1.3m
Bore Hole_ID:K14.1 Lat- 26.17°   Long.-91.75°   **(b)**

Depth (m)	Soil Description	Lithology	N_{obs}	Fines Content %	σ_v (kN/m^2)	σ_v' (kN/m2)	N_{cr}	R_d	CSR	CRR	FS
1.5			8	-	26.16	24.20					
3	Clay upto		19	-	70.27	53.59					
4.5	8m		19	-	114.38	82.99					
6			15	-	158.49	112.38					
7.5			11	-	202.60	141.78					
9			13	-	247.13	171.59	11	0.95	0.34	0.13	0.36
10.5	Silt and Fine		25	4.8	291.85	201.60	19	0.93	0.44	0.19	0.44
12	Sand from		28	4.7	336.56	231.59	20	0.92	0.46	0.21	0.45
13.5	8m to 9m		29	3.6	381.28	261.60	20	0.90	0.46	0.20	0.44
15			26	3.8	425.99	291.59	16	0.89	0.41	0.17	0.41

Reliability approach for soil liquefaction

Deterministic methods rely on the FS for determining the occurrence of liquefaction. The deterministic methods create disparity of results even for the same input parameters. Nevertheless, the abundance of the field data enables the methods quite reliable and is used in most of the assessment. Indeed, it is observed that liquefaction probability could not be established by the calculation of only FS. However, the uncertainty of the parameters causes the inaccuracy in the evaluations of liquefaction potential. Therefore, the necessity to estimate liquefaction probability could be achieved by the application of probabilistic methods or reliability analysis. For developing more substantial result, reliability analysis could be performed for better engineering judgments. Reliability analysis dictates the inclusion of statistical parameters of various inputs in the computations of Reliability Index and eventually liquefaction probability is

Table 2 Typical computation of FS for PGA = 0.36 g corresponding to M_w = 8.1 based on Youd and Idriss [5]

Location :   Rehabari. GWT:1.3m
Bore Hole_ID:K14.1   Lat- 26.17°   Long.-91.75°

| Depth (m)	Soil Description	Lithology	N_{obs}	Fines Content %	σ_v (kN/m²)	σ_v' (kN/m2)	N_{cr}	R_d	CSR	CRR	FS
1.5			8	-	26.16	24.20	12	0.99			
3	Clay upto		19	-	70.27	53.59	19	0.98			
4.5	8m		19	-	114.38	82.99	18	0.97			
6			15	-	158.49	112.38	12	0.95			
7.5			11	-	202.60	141.78	10	0.94			
9			13	-	247.13	171.59	10	0.93	0.31	0.12	0.31
10.5	Silt and Fine		25	4.8	291.85	201.60	18	0.89	0.30	0.20	0.53
12	Sand from		28	4.7	336.56	231.59	19	0.85	0.29	0.21	0.59
13.5	8m to 9m		29	3.6	381.28	261.60	19	0.81	0.28	0.20	0.59
15			26	3.8	425.99	291.59	16	0.77	0.26	0.17	0.53
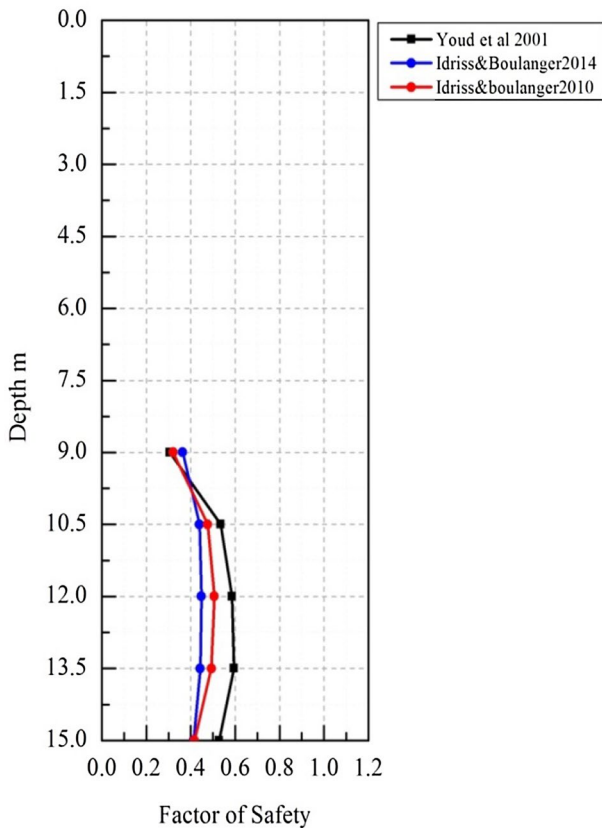
Fig. 4 FS comparison between Youd and Idriss [5] and Idriss and Boulanger [2, 6] presented for the study area

evaluated. In reliability approach, the first step is to determine performance function. If the performance function values of definite portions of the entire structure surpass beyond a definite value under a given load, it is assumed that the structure would fail if it cannot satisfy the required condition. The condition is known as the limit state performance function of the system. In the deterministic liquefaction evaluation methods, if the CSR is denoted as S and the CRR is denoted as R, it could be described that the performance function for soil liquefaction is $Z = R - S$. The performance function Z compares the parameters of CRR and CSR to evaluate the liquefaction susceptibility. Thus, it could be assumed that if $Z = R - S < 0$, the performance state is designated as 'failed', i.e., liquefaction happens. If $Z = R - S > 0$, the performance state is designated as 'safe', i.e., no liquefaction occurs. If $Z = R - S = 0$, the performance state is labeled as a 'limit state', i.e., on the margin between liquefaction and non-liquefaction conditions. It is observed that there is some inherent error involved in the estimation of the CSR and also in the CRR; if we consider CRR as R and CSR as S to be random variables, then the liquefaction state performance function would also be a random variable. Therefore, considering the probability of occurrence, the above three performance states could be estimated. The probability of occurrence of liquefaction is defined as the probability that limits state performance function which becomes, $Z = R - S \leq 0$. Nevertheless, a precise computation of this probability is not simple. In reality, the determination

of probability density function of CSR and CRR is complex: Furthermore, the computation of the liquefaction probability of $Z = R - S \leq 0$ needs multiple integrations over the CRR and CSR domains, which is a complex and tiresome process.

First-order second-moment (FOSM)

FOSM is the commonly used method to compute the performance function because it depends only on the means and standard deviations of a random variables. The method is based on the statistics of the basic independent random variables, such as CRR and CSR to determine the estimated statistics of the limit state performance function, variable, $Z = R - S$, which enables to carry out the operation of the complex integration process in a simpler way. Following the standard of statistics, the liquefaction state performance function $Z = R - S$ is assumed as normally distributed random variable, if CRR and CSR are considered as independent random variables having a normal distribution. Considering the mean values and standard deviations of CRR and CSR as μ_R, μ_S and σ_R, σ_S, respectively, then, according to the FOSM, the mean value, μ_z, the standard deviation, σ_z, and the coefficient of variation (COV), δ_z, of Z could be expressed as:

$$\mu_z = \mu_R - \mu_S, \tag{18}$$

$$\sigma_z = \sqrt{\sigma_R^2 + \sigma_S^2}, \tag{19}$$

$$\delta_z = \frac{\sigma_Z}{\mu_Z}, \tag{20}$$

The Reliability Index β which is the inverse of the COV δ_Z is defined as:

$$\frac{\mu_Z}{\sigma_Z} = \frac{\sqrt{\sigma_R^2 + \sigma_S^2}}{\mu_R - \mu_s}. \tag{21}$$

Reliability Index β is used to measure the reliability of liquefaction assessment results. It is often observed that basic engineering random variables normally consist of non-zero values and are usually slightly skewed; therefore, it could be described more accurately by log-normal distribution model (Rosenblueth and Estra 1972). Reliability Index in terms of logarithmic variables is expressed as [6]:

$$\beta = \frac{\ln\left[\frac{\mu_{\text{CRR}}}{\mu_{\text{CSR}}} \frac{\sqrt{\delta_{\text{CSR}}^2 + 1}}{\sqrt{\delta_{\text{CRR}}^2 + 1}}\right]}{\sqrt{\ln\left[(\delta_{\text{CRR}}^2 + 1)(\delta_{\text{CSR}}^2 + 1)\right]}}. \tag{22}$$

The risk in term of liquefaction probability P_{L} can be obtained from the Reliability Index β by:

$$P_{\text{L}} = 1 - \phi(\beta), \tag{23}$$

where $\phi(\beta)$ is the normal cumulative probability distribution of random variables.

The FS could be evaluated using the equation:

$$\text{FS} = \frac{\mu_R}{\mu_S}. \tag{24}$$

Re-arranging Eqs. (23) and (25), the following expression can be obtained:

$$\beta = \frac{\ln\left[\text{FS} \cdot \frac{\sqrt{\delta_{\text{CSR}}^2 + 1}}{\sqrt{\delta_{\text{CRR}}^2 + 1}}\right]}{\sqrt{\ln[(\delta_{\text{CRR}}^2 + 1)(\delta_{\text{CSR}}^2 + 1)]}}. \tag{25}$$

The above equation could be used to calculate Reliability Index corresponding to a FS and also subsequently evaluate the liquefaction probability.

Uncertainties in CSR

The CSR is the stress or loading developed in the soil due to an earthquake. It could be observed that the influence of PGA plays an important role in its determination. The variability in CSR is mainly due to the uncertainties in the ground acceleration. As per simplified method, CSR is given as:

$$\text{CSR} = 0.65 \left(\frac{\sigma_{\text{vo}} A_{\text{max}}}{\sigma_{\text{vo}}' g}\right) \frac{r_{\text{d}}}{\text{MSF}} \cdot \frac{1}{K_\sigma}. \tag{26}$$

The FOSM method uses a Taylor series expansion of the function to be calculated. The expansion is reduced after the first-order terms due to which the accuracy of the method deteriorates if second and higher derivatives of the function are significant. Using this FOSM method, the mean and COV of CSR is given by:

$$\mu_{\text{CSR}} = 0.65 \frac{\mu_a \max}{g} \cdot \frac{\mu_{\sigma_{\text{vo}}}}{\mu_{\sigma_{\text{vo}}'}} \cdot \frac{\mu_{r_{\text{d}}}}{\mu_{\text{MSF}}} \cdot \frac{1}{\mu_{K_\sigma}}, \tag{27}$$

$$\delta_{\text{CSR}}^2 = \delta_a^2 \max + \delta_{\sigma_{\text{vo}}'}^2 + \delta_{\sigma_{\text{vo}}}^2 + \delta_{r_{\text{d}}}^2 + \delta_{\text{MSF}}^2 + \delta_{K_\sigma}^2 - 2\rho_{\sigma_{\text{vo}}' \cdot \sigma_{\text{vo}}} \delta_{\sigma_{\text{vo}}'} \delta_{\sigma_{\text{vo}}}, \tag{28}$$

where μ and V represent the corresponding mean and COV (ratio of standard deviation to mean), respectively, and $\rho_{\sigma_{\text{vo}}' \cdot \sigma_{\text{vo}}}$ represents the correlation coefficient between total and effective stress.

Uncertainties in CRR

The resistance of the soil against soil liquefaction is evaluated based on in situ SPT-N values. In the computation of CRR the adjusted N values are very crucial. A corrected N value involves several procedural correction factors such as overburden correction, energy correction, borehole correction, rod length correction, and sample correction, which increase the uncertainties. It could be observed that the performance of SPT in the field yields some measurement error, if the uncertainties from procedural corrections and measurement errors are considered then the net uncertainties in the evaluation of N values become higher.

The mean of CRR could be calculated using Eqs. (7) and (16) for both the methods using the mean value of $(N_1)_{60cs}$. The COV could be computed as formulated Jha and Suzuki [7]:

$$\delta_{CRR} = \frac{\Delta CRR}{2\mu_{CRR}}, \tag{29}$$

w h e r e $\Delta C R R = CRR_{(\mu(N_1)60cs+\sigma(N_1)60cs)} - CRR_{(\mu(N_1)60cs-\sigma(N_1)60cs)}$, $\mu_{(N_1)60cs}$ is the mean of corrected N values and $\sigma_{(N_1)60cs}$ is the standard deviation of corrected N values

In this study, based on the SPT-N data collected and evaluation of liquefaction potential using the methods by Idriss and Boulanger [2, 6] and Youd and Idriss [5], the following input parameters are calculated for performing reliability analysis.

The coefficient correlation $\rho_{\sigma_v \cdot \sigma'_v}$ between σ_v and σ'_v has been calculated based on Pearson's method and found to be 0.998. The computation of COV for MSF and r_d for both the model is based on three sigma rule [26, 27]. The COV for PGA is assumed as 0.16 corresponding to M_w 8.1 as per [28]. Using the input parameters given in Table 3, the COV of CSR and CRR is calculated using Eqs. (28) and (29), respectively. Using FOSM, the probability of failure is calculated for both the methods. The computed liquefaction

probability based on FS using Idriss and Boulanger [2, 6] and Youd and Idriss [5] is shown in Tables 4 and 5.

Results and discussion

In this study, FS considered is one, i.e., FS > 1 represents non-liquefiable and FS ≤ 1 are liquefiable. The FS was computed for all the sites at a depth interval of 1.5 m. However, Fig. 5 shows the FS calculated at various depths. However, it could be observed that the FS computed using both the methods shows variations, Youd and Idriss's method [5] shows a lower FS than Idriss and Boulanger's [2, 6] at most of the depth layers. Idriss and Boulanger [6] have shown slightly higher value for FS compared to Idriss and Boulanger [2]. Range of FS for Idriss and Boulanger [6] was (0.226–3.665), for Idriss and Boulanger [2] it was found to be (0.211–2.646) whereas for Youd and Idriss [5] it varies between 0.128 and 1.259. The assessment reveals that a total of 32 sites become prone to soil liquefaction. It could also be established that at the depth below 1.5 m up to 9 m soil layers prone to liquefaction is minimal. The area alongside of GS road, Panbazar, Bharalumukh, Jalukbari and Pandu indicates a high risk of soil liquefaction. Reliability analysis is based on FOSM performed for the assessment of liquefaction potential considering Idriss and Boulanger [2, 6] and Youd and Idriss [5] models. A Reliability Index is evaluated for all the sites and the corresponding liquefaction probability is established. From the reliability analysis, it could be observed from Tables 4a, b and 5 that even at FS > 1, the percentage of liquefaction probability is high, but it should be noted that the derived liquefaction probability is evaluated without including the probability of occurrence of an earthquake of a particular magnitude. Therefore, the actual liquefaction probability is the probability that liquefaction would occur during an earthquake if it takes into account the probability of earthquake occurrence and its magnitude. The availability of SPT data attributes to the overall quality of the assessment; hence, a vast data should be employed

Table 3 Input parameters for reliability analysis

Input parameters	Youd and Idriss [5]		Idriss and Boulanger [6]		Idriss and Boulanger [2]	
	Mean	COV	Mean	COV	Mean	COV
a_{max}	0.36	0.16	0.36	0.16	0.36	0.16
σ_v	244.58	0.58	244.58	0.58	244.58	0.58
σ_v	167.52	0.56	167.52	0.56	167.52	0.56
r_d	0.909	0.075	0.948	0.035	0.948	0.035
MSF	0.859	0.27	0.859	0.27	0.198	0.22
$(N_1)_{60cs}$	16	0.343	17	0.326	17	0.326
K_σ	–	–	0.96	0.091	0.96	0.091

Table 4 Typical liquefaction probability using FOSM method (a) Idriss and Boulanger [2], (b) Idriss and Boulanger [6]

BH_ID	Depth (m)	CSR	CRR	FOS	β	P_f %	BH_ID	Depth (m)	CSR	CRR	FOS	β	P_f %
FOSM method (a) Idriss and Boulanger [2]													
K2.1	1.5	0.288	0.084	0.292	− 2.73	99.68	74.1	9	0.368	0.161	0.439	− 1.82	96.58
K2.1	9	0.344	0.110	0.319	− 2.54	99.44	74.1	10.5	0.513	0.292	0.570	− 1.24	89.33
46.1	1.5	0.354	0.118	0.334	− 2.43	99.25	74.1	12	0.548	0.328	0.599	− 1.13	87.13
k72.1	15	0.427	0.185	0.433	− 1.85	96.82	74.1	13.5	0.392	0.171	0.437	− 1.83	96.66
k7.1	1.5	0.214	0.075	0.352	− 2.32	98.98	74.1	15	0.483	0.244	0.505	− 1.51	93.47
k7.1	15	0.631	0.541	0.857	− 0.34	63.20	80.1	10.5	0.373	0.149	0.399	− 2.03	97.90
k10.1	1.5	0.251	0.140	0.557	− 1.29	90.20	80.1	12	0.430	0.190	0.442	− 1.81	96.49
k10.1	3	0.233	0.142	0.609	− 1.10	86.38	80.1	13.5	0.407	0.174	0.427	− 1.89	97.03
k10.1	4.5	0.280	0.126	0.452	− 1.76	96.07	80.1	15	0.436	0.195	0.448	− 1.78	96.25
k10.1	6	0.332	0.153	0.461	− 1.72	95.69	k3.1	10.5	0.348	0.120	0.345	− 2.36	99.08
k10.1	7.5	0.347	0.151	0.437	− 1.83	96.66	k3.1	12	0.454	0.197	0.435	− 1.84	96.73
33.1	1.5	0.251	0.140	0.557	− 1.29	90.22	k28.1	10.5	0.337	0.114	0.339	− 2.40	99.18
33.1	3	0.311	0.148	0.476	− 1.65	95.01	k28.1	12	0.500	0.241	0.482	− 1.61	94.67
k14.1	9	0.344	0.125	0.363	− 2.24	98.76	k28.1	13.5	0.481	0.221	0.460	− 1.72	95.74
k14.1	10.5	0.437	0.192	0.439	− 1.82	96.58	k28.1	15	0.523	0.256	0.489	− 1.58	94.35
k14.1	12	0.461	0.207	0.448	− 1.78	96.22	196	7.5	0.515	0.249	0.484	− 1.61	94.60
k14.1	13.5	0.457	0.202	0.443	− 1.80	96.43	88	1.5	0.460	0.374	0.812	− 0.46	67.58
k14.1	15	0.407	0.168	0.413	− 1.96	97.50	85	4.5	0.347	0.147	0.424	− 1.90	97.14
42.1	1.5	0.195	0.075	0.385	− 2.12	98.29	37	9	0.410	0.174	0.424	− 1.90	97.13
k18.3	1.5	0.300	0.092	0.307	− 2.62	99.56	37	10.5	0.430	0.194	0.451	− 1.76	96.09
k30.1	12	0.446	0.186	0.417	− 1.94	97.38	22	1.5	0.237	0.050	0.211	− 3.45	99.97
k30.1	13.5	0.350	0.119	0.339	− 2.40	99.17	22	12	0.447	0.188	0.421	− 1.92	97.25
k30.1	15	0.355	0.125	0.354	− 2.30	98.94	22	13.5	0.607	0.482	0.793	− 0.51	69.44
58.2	1.5	0.289	0.075	0.260	− 2.99	99.86	22	15	0.411	0.164	0.399	− 2.04	97.93
58.2	3	0.338	0.120	0.354	− 2.30	98.93	75.1	4.5	0.526	0.649	1.234	0.47	31.82
34.1	10.5	0.389	0.162	0.417	− 1.94	97.38	75.1	7.5	0.442	0.198	0.448	− 1.78	96.22
34.1	12	0.389	0.160	0.412	− 1.97	97.54	91.1	9	0.447	0.209	0.468	− 1.68	95.39
34.1	13.5	0.437	0.195	0.447	− 1.78	96.28	91.1	10.5	0.422	0.186	0.440	− 1.82	96.56
34.1	15	0.580	0.339	0.584	− 1.19	88.31	91.1	12	0.434	0.193	0.445	− 1.80	96.37
53.1	1.5	0.223	0.098	0.440	− 1.82	96.55	92.1	4.5	0.444	0.242	0.544	− 1.35	91.10
53.1	3	0.263	0.092	0.349	− 2.33	99.01	92.1	6	0.305	0.086	0.282	− 2.80	99.75
53.1	13.5	0.483	0.233	0.482	− 1.61	94.67	92.1	7.5	0.520	0.284	0.545	− 1.34	91.02
53.1	15	0.519	0.268	0.517	− 1.46	92.82	30	1.5	0.214	0.075	0.352	− 2.32	98.98
83.1	9	0.340	0.115	0.338	− 2.41	99.20	29	1.5	0.287	0.118	0.412	− 1.97	97.53
62.3	13.5	0.425	0.184	0.432	− 1.86	96.86	26	1.5	0.315	0.219	0.693	− 0.81	79.04
62.3	15	0.442	0.194	0.440	− 1.82	96.56	24	1.5	0.307	0.125	0.407	− 1.99	97.67
71.1	1.5	0.334	0.125	0.375	− 2.17	98.51	112	9	0.534	0.249	0.467	− 1.69	95.41
78.1	10.5	0.408	0.171	0.419	− 1.93	97.31	112	10.5	0.631	1.670	2.646	2.17	1.50
78.1	12	0.398	0.164	0.411	− 1.97	97.57	112	12	0.642	0.759	1.181	0.38	35.32
78.1	13.5	0.404	0.168	0.417	− 1.94	97.37	112	13.5	0.651	0.644	0.989	− 0.02	50.71
78.1	15	0.378	0.146	0.387	− 2.10	98.23	112	15	0.659	0.644	0.977	− 0.05	51.83
FOSM method (b) Idriss and Boulanger [6]													
K2.1	1.5	0.362	0.084	0.233	− 3.23	99.94	74.1	9	0.371	0.161	0.435	− 1.84	96.74
K2.1	9	0.407	0.110	0.270	− 2.91	99.82	74.1	10.5	0.387	0.292	0.755	− 0.62	73.23
46.1	1.5	0.409	0.118	0.289	− 2.76	99.71	74.1	12	0.396	0.328	0.828	− 0.41	65.99
k72.1	15	0.402	0.185	0.460	− 1.72	95.74	74.1	13.5	0.384	0.171	0.446	− 1.79	96.30
k7.1	1.5	0.272	0.075	0.276	− 2.85	99.78	74.1	15	0.395	0.244	0.618	− 1.06	85.60
k7.1	15	0.455	0.541	1.189	0.39	34.79	80.1	10.5	0.392	0.149	0.380	− 2.14	98.39
k10.1	1.5	0.272	0.140	0.515	− 1.47	92.89	80.1	12	0.399	0.190	0.476	− 1.64	94.99

Table 4 (continued)

BH_ID	Depth (m)	CSR	CRR	FOS	β	P_f %	BH_ID	Depth (m)	CSR	CRR	FOS	β	P_f %
k10.1	3	0.250	0.142	0.567	−1.26	89.54	80.1	13.5	0.396	0.174	0.439	−1.82	96.59
k10.1	4.5	0.315	0.126	0.401	−2.02	97.85	80.1	15	0.399	0.195	0.490	−1.58	94.31
k10.1	6	0.344	0.153	0.445	−1.80	96.37	k3.1	10.5	0.400	0.120	0.300	−2.67	99.62
k10.1	7.5	0.361	0.151	0.420	−1.92	97.28	k3.1	12	0.412	0.197	0.479	−1.63	94.84
33.1	1.5	0.272	0.140	0.515	−1.47	92.92	k28.1	10.5	0.394	0.114	0.290	−2.74	99.70
33.1	3	0.328	0.148	0.451	−1.76	96.12	k28.1	12	0.411	0.241	0.587	−1.18	88.06
k14.1	9	0.390	0.125	0.321	−2.52	99.41	k28.1	13.5	0.412	0.221	0.537	−1.38	91.56
k14.1	10.5	0.403	0.192	0.477	−1.64	94.96	k28.1	15	0.418	0.256	0.611	−1.09	86.15
k14.1	12	0.409	0.207	0.505	−1.51	93.48	196	7.5	0.417	0.249	0.597	−1.14	87.27
k14.1	13.5	0.410	0.202	0.494	−1.56	94.08	88	1.5	0.331	0.374	1.129	0.28	39.15
k14.1	15	0.403	0.168	0.417	−1.94	97.36	85	4.5	0.367	0.147	0.400	−2.03	97.87
42.1	1.5	0.248	0.075	0.303	−2.65	99.60	37	9	0.399	0.174	0.436	−1.84	96.71
k18.3	1.5	0.370	0.092	0.249	−3.09	99.90	37	10.5	0.394	0.194	0.493	−1.57	94.13
k30.1	12	0.418	0.186	0.444	−1.80	96.39	22	1.5	0.302	0.050	0.166	−3.99	100.00
k30.1	13.5	0.404	0.119	0.294	−2.72	99.67	22	12	0.417	0.188	0.451	−1.76	96.10
k30.1	15	0.401	0.125	0.313	−2.58	99.50	22	13.5	0.437	0.482	1.102	0.22	41.23
58.2	1.5	0.368	0.075	0.204	−3.53	99.98	22	15	0.412	0.164	0.397	−2.05	97.96
58.2	3	0.389	0.120	0.308	−2.61	99.55	75.1	4.5	0.379	0.649	1.712	1.20	11.48
34.1	10.5	0.392	0.162	0.413	−1.96	97.49	75.1	7.5	0.401	0.198	0.495	−1.56	94.05
34.1	12	0.395	0.160	0.406	−2.00	97.72	91.1	9	0.394	0.209	0.530	−1.40	91.99
34.1	13.5	0.400	0.195	0.489	−1.59	94.36	91.1	10.5	0.396	0.186	0.469	−1.68	95.34
34.1	15	0.418	0.339	0.810	−0.46	67.81	91.1	12	0.399	0.193	0.484	−1.61	94.62
53.1	1.5	0.272	0.098	0.361	−2.26	98.80	92.1	4.5	0.364	0.242	0.664	−0.91	81.74
53.1	3	0.325	0.092	0.283	−2.80	99.74	92.1	6	0.381	0.086	0.226	−3.30	99.95
53.1	13.5	0.403	0.233	0.578	−1.21	88.71	92.1	7.5	0.398	0.284	0.713	−0.75	77.24
53.1	15	0.407	0.268	0.659	−0.92	82.16	30	1.5	0.272	0.075	0.276	−2.85	99.78
83.1	9	0.397	0.115	0.289	−2.75	99.70	29	1.5	0.331	0.118	0.357	−2.29	98.89
62.3	13.5	0.402	0.184	0.457	−1.73	95.86	26	1.5	0.272	0.219	0.804	−0.48	68.40
62.3	15	0.405	0.194	0.480	−1.63	94.81	24	1.5	0.348	0.125	0.360	−2.27	98.83
71.1	1.5	0.378	0.125	0.331	−2.45	99.29	112	9	0.432	0.249	0.577	−1.22	88.79
78.1	10.5	0.400	0.171	0.427	−1.88	97.03	112	10.5	0.455	1.670	3.669	2.90	0.19
78.1	12	0.400	0.164	0.409	−1.98	97.63	112	12	0.463	0.759	1.639	1.10	13.47
78.1	13.5	0.399	0.168	0.422	−1.91	97.20	112	13.5	0.469	0.644	1.374	0.71	23.83
78.1	15	0.401	0.146	0.365	−2.23	98.73	112	15	0.475	0.644	1.356	0.68	24.72

for the detailed assessment. A typical comparison of FS evaluated based on recent and earlier model of Idriss and Boulanger [2, 6] has been prepared as shown in Fig. 5. It could be seen that the revised MSF as given in Idriss and Boulanger [2] appears to have caused the conservation of FS as compared to its earlier model. Considering the available data of the study area, a liquefaction probability curve corresponding to FS for all the boreholes is prepared as shown in Fig. 6. Indeed, it has been observed that Youd and Idriss's [5] model shows a high liquefaction probability (FS > 1) while comparing with the Idriss and Boulanger's [2, 6]; however, when FS < 1, Idriss and Boulanger's [2] model shows slightly higher probability comparing with the Youd and Idriss's [5]. However, it could be concluded

that in estimating liquefaction probability (FS < 1), both the methods could be used to attain reliable results.

However, authors (Singhnar and Sil 2017) have conducted studies considering FS and LPI, the result is presented in the form of contour maps as spatial variation of FS along the depth-wise variations [considering the types of foundation of various structures such as shallow and deep that normally varies up to 3–15 m] showing the vulnerable locations/areas in Guwahati city. The contour map based on a FS at various depths (3 and 15 m) is shown in Fig. 7a, b, respectively. It could be observed from the map that at a depth of 3 m, (shown in Fig. 7a), the FS of all the 82 locations reveals that an area comprising Pandu, Kamakhya in the North-west, Rehabari, Ulubari at the central, and Madhgharia, RG

Table 5 Typical calculations of liquefaction probability using FOSM method [5]

BH_ID	Depth (m)	CSR	CRR	FOS	β	P_f %	BH_ID	Depth (m)	CSR	CRR	FOS	β	P_f %
K2.1	1.5	0.338	0.053	0.128	−4.43	100.00	78.1	12	0.295	0.187	0.520	−1.42	92.29
K2.1	9	0.329	0.088	0.219	−3.29	99.95	78.1	13.5	0.282	0.197	0.572	−1.22	88.88
46.1	1.5	0.348	0.131	0.309	−2.55	99.45	78.1	15	0.268	0.224	0.685	−0.83	79.71
k72.1	15	0.267	0.196	0.602	−1.11	86.63	74.1	9	0.301	0.191	0.521	−1.42	92.19
k7.1	1.5	0.231	0.053	0.188	−3.62	99.99	74.1	10.5	0.293	0.368	1.031	0.05	48.06
k7.1	15	0.271	0.313	0.946	−0.13	55.35	74.1	12	0.283	0.410	1.188	0.36	36.11
k10.1	1.5	0.231	0.141	0.498	−1.52	93.53	74.1	13.5	0.272	0.200	0.602	−1.11	86.61
k10.1	3	0.229	0.145	0.521	−1.42	92.24	74.1	15	0.261	0.289	0.910	−0.22	58.66
k10.1	4.5	0.275	0.124	0.369	−2.16	98.47	80.1	10.5	0.301	0.159	0.434	−1.81	96.50
k10.1	6	0.292	0.165	0.462	−1.68	95.34	80.1	12	0.289	0.208	0.590	−1.15	87.54
k10.1	7.5	0.300	0.163	0.446	−1.76	96.05	80.1	13.5	0.276	0.189	0.563	−1.25	89.50
33.1	1.5	0.231	0.192	0.680	−0.85	80.14	80.1	15	0.263	0.212	0.660	−0.91	81.87
33.1	3	0.300	0.192	0.524	−1.41	92.03	k3.1	10.5	0.307	0.113	0.302	−2.60	99.53
k14.1	9	0.314	0.117	0.305	−2.57	99.49	k3.1	12	0.294	0.192	0.535	−1.36	91.38
k14.1	10.5	0.303	0.197	0.535	−1.36	91.38	k28.1	10.5	0.307	0.111	0.297	−2.63	99.57
k14.1	12	0.290	0.207	0.585	−1.17	87.91	k28.1	12	0.294	0.253	0.706	−0.77	77.79
k14.1	13.5	0.277	0.201	0.595	−1.13	87.17	k28.1	13.5	0.281	0.225	0.656	−0.92	82.22
k14.1	15	0.264	0.170	0.528	−1.39	91.82	k28.1	15	0.267	0.246	0.754	−0.62	73.33
42.1	1.5	0.231	0.053	0.188	−3.62	99.99	196	7.5	0.342	0.292	0.700	−0.78	78.31
k18.3	1.5	0.315	0.117	0.305	−2.57	99.49	88	1.5	0.282	0.203	0.591	−1.15	87.44
k30.1	12	0.310	0.202	0.535	−1.36	91.38	85	4.5	0.320	0.141	0.360	−2.21	98.66
k30.1	13.5	0.293	0.120	0.336	−2.37	99.10	37	9	0.324	0.318	0.805	−0.48	68.56
k30.1	15	0.279	0.131	0.387	−2.06	98.03	37	10.5	0.302	0.313	0.850	−0.37	64.31
58.2	1.5	0.341	0.053	0.188	−3.62	99.99	22	1.5	0.282	0.053	0.154	−4.05	100.00
58.2	3	0.345	0.113	0.395	−2.02	97.81	22	12	0.309	0.215	0.572	−1.22	88.87
34.1	10.5	0.302	0.185	0.502	−1.50	93.31	22	15	0.279	0.192	0.563	−1.25	89.47
34.1	12	0.289	0.171	0.485	−1.57	94.22	75.1	7.5	0.326	0.217	0.545	−1.32	90.69
34.1	13.5	0.277	0.209	0.620	−1.04	85.19	91.1	9	0.316	0.268	0.696	−0.80	78.67
34.1	15	0.263	0.309	0.963	−0.10	53.90	91.1	10.5	0.305	0.221	0.594	−1.14	87.24
53.1	1.5	0.231	0.104	0.370	−2.16	98.45	91.1	12	0.293	0.198	0.554	−1.29	90.11
53.1	3	0.290	0.088	0.248	−3.02	99.87	92.1	4.5	0.318	0.309	0.799	−0.50	69.12
53.1	13.5	0.278	0.235	0.692	−0.81	79.05	92.1	6	0.320	0.087	0.223	−3.25	99.94
53.1	15	0.265	0.256	0.792	−0.52	69.77	92.1	7.5	0.320	0.492	1.259	0.48	31.55
83.1	9	0.321	0.115	0.358	−2.23	98.71	30	1.5	0.231	0.053	0.188	−3.62	99.99
62.3	13.5	0.190	0.191	0.822	−0.44	66.91	29	1.5	0.282	0.230	0.668	−0.88	81.18
62.3	15	0.181	0.203	0.918	−0.20	57.89	26	1.5	0.181	0.228	1.032	0.05	47.90
71.1	1.5	0.321	0.113	0.426	−1.85	96.82	24	1.5	0.296	0.269	0.745	−0.65	74.19
78.1	10.5	0.309	0.198	0.525	−1.40	91.98	112	9	0.344	0.370	0.654	−0.93	82.39

Baruah road in the northeastern region of the city is found to be vastly susceptible to liquefaction.

Similarly, at higher depth such as 15 m presented in figure 7(b), it could be observed that the areas including Bamunimaidan, Noomati, R G Baruah road in the northeastern part, adjacent areas of Pandu in the west and areas surrounding Rehabari in the central part of Guwahati city found to be still susceptible to liquefaction. Hence, soil site investigation for liquefaction is highly recommended for such area.

However, the soil LPI is estimated and presented in the form of contour map (Fig. 7c, d) showing the level of severity of liquefaction at various depths (3 and 15 m) along with borehole locations. The computed value of LPI for Guwahati city ranges from 0 to 33 covering at a depth of 15 m. From the contour map shown in figure, the severity of liquefaction at a depth of 3 m for all the 82 borehole locations reveals a very high risk of liquefaction (LPI > 15) in the area comprising Bamunimaidan located in the northeastern part of the city. The Northwestern, some part of the central area and
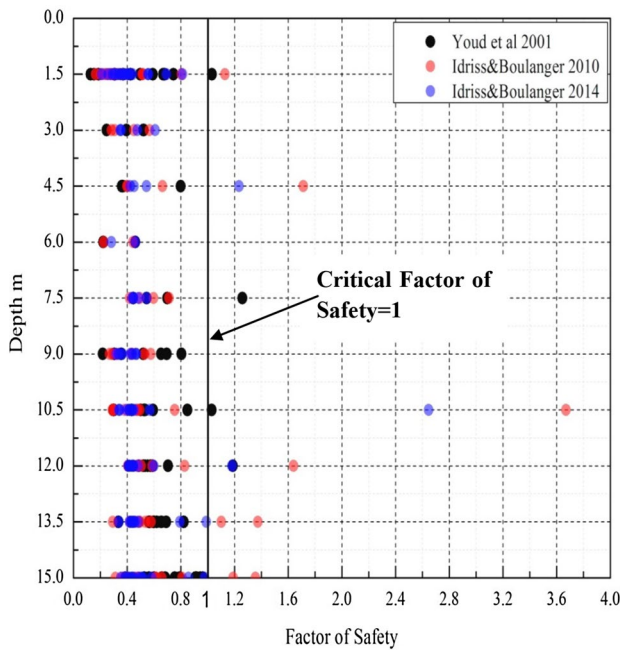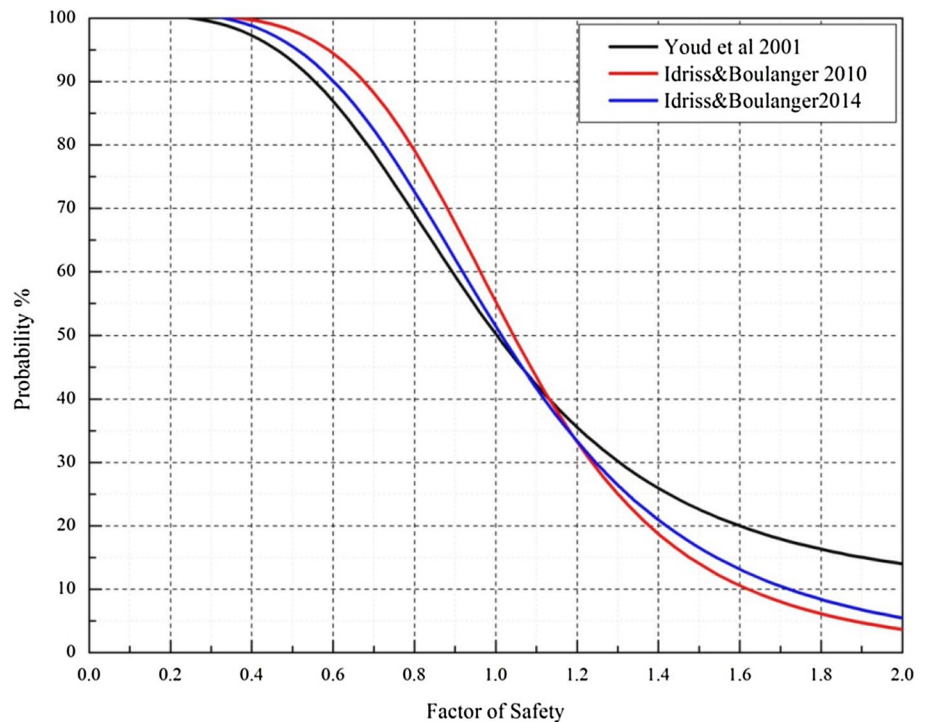
Fig. 5 FS along depths of all the selected sites

northeastern part of the city have the high risk of liquefaction (15 > LPI > 5) whereas large area located in the southern part of the city has low severity. At a depth 15 m, it could be observed that the of severity of liquefaction is similar to some areas falling in the very high risk category such as the area neighboring AT Road, Bamunimaidan, Madhgharia

located in the central north, and northeastern part of the city, respectively. The liquefaction hazard maps based on FOS against soil liquefaction and LPI could be used to evaluate the severity and identification of liquefaction sites for construction in Guwahati city, and suitable foundation or corrective soil improvement measures could be adopted for further strengthening of soil against the liquefaction failure in future events in the study area.

According to the study carried out by Raghukanth and Dash [29], also supports this study, however, authors have made an attempt to represent the results with the updated available in situ subsurface test data and methods, by estimating and showing FOS, indeed, LPI with the variations along depths through a probabilistic approach considering the severity and importance of the city on priority for seismic safety during future events as a precautionary measure.

Conclusions

The extent of damage due to soil liquefaction that was witnessed in Niigata earthquake and Alaska earthquake event in 1964 has caused a great concern for geotechnical engineers. Since then, several researchers have been studying to evaluate liquefaction susceptibility and its dynamic characteristics. In this study, an attempt has been made to evaluate the liquefaction potential of Guwahati city through reliability approach. The assessment of soil liquefaction for Guwahati city is carried out using the

Fig. 6 Liquefaction probability curve using FOSM

Fig. 7 **a**, **b** Typical map showing spatial variation of FOS against liquefaction of Guwahati city at a depth of 3 and 15 m, respectively. **c**, **d** Map showing spatial variation of LPI of Guwahati city at a depth of 3 and 15 m, respectively
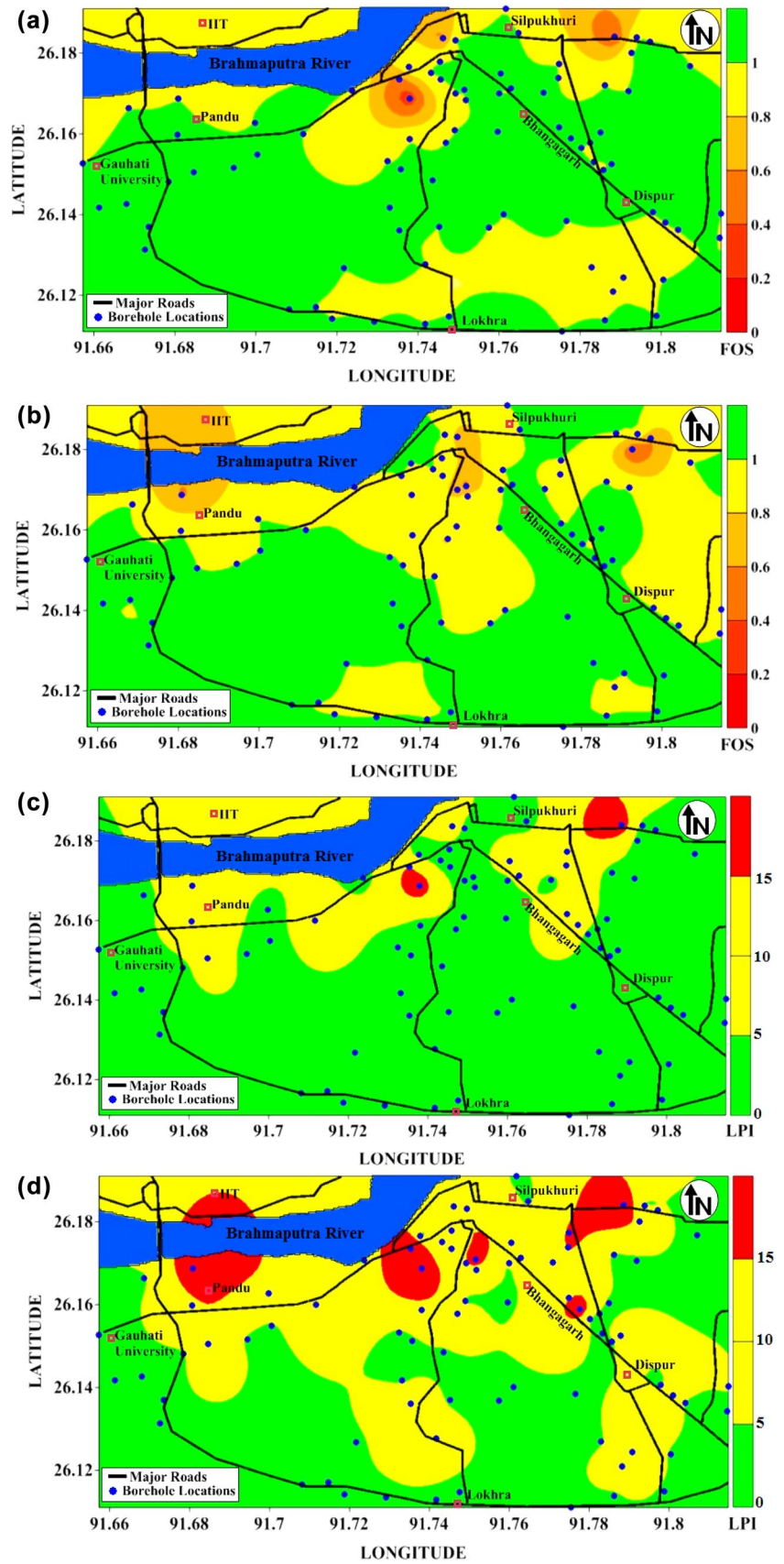
method proposed by Youd and Idriss [5] and Idriss and Boulanger [2, 6]. A design PGA of 0.36 g for Zone-V as per IS 1893 (part 1):2002 is used considering Great Shillong earthquake 1897 to have occurred generating a magnitude M_w 8.1; however, in the real earthquake scenario, the actual PGA value may vary depending on the earthquake magnitude, local site response, etc., thereby making PGA value very crucial in the liquefaction assessment. It could be established from the results that both the models employed for liquefaction evaluations depict unlike results despite the same inputs. The requirement for more substantial result could be established by reliability analysis which could provide more elaborate information in carrying out engineering works. Reliability analysis using FOSM is performed for both the models and the relationship between FS and liquefaction probability is established. The resultant liquefaction probability, however, does not include the probability that an earthquake of the given magnitude would occur. Nevertheless, the liquefaction probability corresponding to a FS could be used for determining better engineering decisions. In this study, the assessment carried out based on semi-empirical relations using SPT is simpler, but it has some limitations such as the uncertainties involved in various factors used in the evaluation of cyclic stress and cyclic strength of the soil. Therefore, performing reliability analysis enables us to ascertain variation of the parameters and account for the difference of the methods as well. Hence, both deterministic and reliability approaches should be carried out for determining better engineering decisions.

References

1. Seed HB, Idriss IM (1971) Simplified procedure for evaluating soil liquefaction potential. J soil Mech Found Eng ASCE 97(SM9):1249–1273
2. Idriss IM, Boulanger RW (2014) CPT and SPT based liquefaction triggering procedures
3. Seed HB, Idriss IM, Arango I (1983) Evaluation of liquefaction potential using field performances data. J Geotech Eng ASCE 109(3):458–483
4. Seed HB, Tokimatsu K, Harder LF, Chung RM (1985) Influence of SPT procedures in soil liquefaction resistance evaluations. J Geotech Eng ASCE 111(12):1425–1445
5. Youd TL, Idriss IM (2001) Liquefaction resistance of soils: summary report from the 1996 NCEER and 1998 NCEER/NSF workshops on the evaluation of liquefaction resistance of soils. J Geotech Geoenviron Eng 127(4):297–313
6. Idriss IM, Boulanger RW (2010) SPT-based liquefaction triggering procedures. Report No. UCD/CGM-10/02. Department of Civil and Environmental Engineering, University of California, USA
7. Phoon KK, Kulhawy FH (1999) Characterization of geotechnical variability. Can Geotech J 1999(36):612–624
8. Duncan J (2000) Factors of safety and reliability in geotechnical engineering. J Geotech Geoenviron Eng 126(4):307–316
9. Hwang JH et al (2004) A practical reliability-based method for assessing soil liquefaction potential. Soil Dyn Earthq Eng (Elsevier) 24(2004):761–770
10. Jha SK, Suzuki K (2008) Reliability analysis of soil liquefaction based on standard penetration test. Comput Geotech (Elsevier) 36(2009):589–596
11. Hough SE, Bilham R, Ambraseys N, Feldl N (2005) Revisiting the 1897 Shillong and 1905 Kangra earthquakes in northern India: site response, Moho reflections and a triggered earthquake. Curr Sci 88(10):1632–1638
12. Youd TL, Hoose SN (1977) Liquefaction susceptibility and geologic setting. In: Proceedings of the 6th world conference on earthquake engineering, New Delhi, India, vol 6, pp 37–42
13. Youd TL, Perkins DM (1978) Mapping liquefaction-induced ground failure potential. J Geotech Eng Div Am Soc Civ Eng 104:433–446
14. Mitchell JK (1986) Practical problems from surprising soil behavior. J Geotech Eng 112(3):259–289
15. Mitchell JK, Solymar ZV (1984) Time-dependent strength gain in freshly deposited or densified sand. J Geotech Eng 110(11):1559–1576
16. Schmertmann JH (1991) The mechanical aging of soils. J Geotech Eng 117(9):1288–1330
17. Sil A, Sitharam TG, Kolathayar S (2013) Probabilistic seismic hazard analysis of Tripura and Mizoram states. Nat Hazards (Springer publication) 68(2):1089–1108
18. Zarola A, Sil A (2018) Forecasting of future earthquakes in the Northeast region of India. Comput Geosci (Elsevier Publication) 113:1–13
19. Zarola A, Sil A (2017) Artificial neural networks (ANN) and stochastic techniques to estimate earthquake occurrences in Northeast region of India. Ann Geophys INGV 60(4):1–37
20. Gupta HK, Singh VP (1980) Teleseismic P-wave residual investigations at Shillong, India. Tectonophysics 66:T19–T29
21. Guha SK, Bhattacharya U (1984) Studies on the prediction of seismicity in northeastern India. In: Presented at the 8th world conference on earthquake engineering, San Francisco, 21–27 July 1984
22. Bilham R, England P (2001) Plateau pop-up during the great 1897 Assam earthquake. Nature (Lond) 410:806–809
23. Seed HB (1979) Soil liquefaction and cyclic mobility evaluation for level ground during earthquakes. J Geotech Eng Div ASCE 105(GT2):201–255
24. Liao SSC, Whitman RV (1986a) Catalogue of liquefaction and non-liquefaction occurrences during earthquakes. Massachusetts Institute of Technology, Cambridge, Mass
25. Liao SC, Whitman RV (1986b) Overburden correction factors for SPT in sand. J GeotechEng ASCE 112(3):373–377
26. Christian JT, Baecher GB (2001) Discussion of Factor of Safety and Reliability in Geotechnical Engineering. J Geotech Geoenviron Eng 127(8):700–703
27. Baecher GB, Christian JT (2001) Reliability and statistics in geotechnicalengineering. Wiley, New York
28. Raghukanth STGR, Dash SK (2010) Evaluation of seismic soil liquefaction at Guwahati city. Environ Earth Sci 2010(61):355–368
29. Raghukanth STG, Dash SK (2008) Stochastic modelling of SPT n-value and evaluation of probability of liquefaction at Guwahati city. J Earthq Tsunami 2(3):175–196